Fragmentation in a ϕ^3-Theory Ladder Model

R. Rajaraman and A. Banerjee
Department of Physics, Delhi University, Delhi-7, India

(Received 3 April 1972; revised manuscript received 19 June 1972)

We study the inclusive reaction $a+b \to c+$ (anything), where all the particles belong to a single scalar field $\phi(x)$ interacting through a $g\phi^3(x)$ term. We do this in a ladder model for the forward $ab\bar{c} \to ab\bar{c}$ process, whose amplitude is intimately related to the inclusive distribution. The choice of the infinite sequence of ladder diagrams as well as the assumptions involved are natural extensions of analogous work in the literature for four-point functions. In the fragmentation limit, the model yields the expected Regge behavior as the initial energy tends to infinity. An expression is derived for the limiting distribution function $E_c\, d\sigma/d\vec{p}_c$ for fixed $\vec{p}_c$ as $s \to \infty$. The results are derived both in the "leading-term approximation" as well as by an exact Mellin-transform method.

I. INTRODUCTION

Inclusive hadronic reactions have been the subject of considerable study in the last few years. In particular, the hypothesis of limiting fragmentation[1] has gained encouraging support both from experiment[2] and from Mueller's O(2, 1) analysis[3] of inclusive reactions, based on a generalized optical theorem.

Model calculations for such phenomena already exist in the literature[4] using both dual theories and multiperipheral amplitudes. In this paper, we study fragmentation using somewhat different techniques, although the physics is closely related to multiperipheral models. As Mueller has shown,[3] the inclusive distribution for the fragment c in the reaction $a+b \to c+$ (anything) is closely related to the forward $ab\bar{c} \to ab\bar{c}$ amplitude. We evaluate, in a ϕ^3 theory, the high-energy $ab\bar{c} \to ab\bar{c}$ amplitude by summing an infinite sequence of crossed-channel ladder graphs. This is done first in the "leading-term approximation" (Sec. II) followed by a more exact result using Mellin-transform techniques (Sec. III). In both cases, the $ab\bar{c} \to ab\bar{c}$ amplitude Reggeizes in the Mueller sense in the fragmentation domain. Further, the Regge trajectories that appear are the same as those that would occur in the same ϕ^3 theory for the elastic $2 \to 2$ amplitudes. This Regge behavior and the identification with the elastic trajectory functions supports Mueller's results, and leads to limiting fragmentation. Our method does not require any additional assumptions about transverse momenta, or about correlations or the absence thereof, between particles widely separated on the rapidity axis.

We also obtain an expression for the limiting distribution $E_c d\sigma/dp_c\,(s \to \infty)$, as a function of p_c. It is shown that this distribution is uniquely obtained in the Mellin-transform method, but not in the simpler leading-term approximation although the latter also yields limiting fragmentation. The residue of the leading Regge pole also factorizes nicely in the sense described in Sec. III.

All the work below follows methods already developed in the literature[5,6] for the "elastic case." By the phrase "elastic case" we will always refer to similar crossed-channel ladder summations for the two-body forward elastic amplitude (four-point functions) in ϕ^3 theory. We will assume familiarity on the reader's part with such methods for the elastic case, and arguments or steps formally identical to the elastic case will be given only in condensed form. Stress will be laid instead on those special features that are introduced in the adaptation of these methods to our $ab\bar{c} \to ab\bar{c}$ process.

At the end of Sec. III, we give a discussion of the choice of graphs that define our model. Some alternate choices are also discussed.

II. LEADING-TERM APPROXIMATION

We treat the process $a(p_a)+b(p_b) \to c(p_c)+$ (anything), where all the particles correspond to the same neutral scalar field $\phi(x)$ of mass μ, interacting through a $g\phi^3(x)$ Hamiltonian. Throughout this paper, we are interested in the fragmentation domain, where p_c is fixed in the laboratory frame of b, as $(E_a)_{\text{lab}}$ tends to infinity (Fig. 1). Let

$$s \equiv (p_a+p_b)^2, \quad s' \equiv (p_a-p_c)^2,$$

$$t \equiv (p_b-p_c)^2 = -2\mu(E_c)_{\text{lab}} + 2\mu^2,$$

$$M^2 \equiv (p_a+p_b-p_c)^2.$$

As $s \to \infty$ for fixed $(\vec{p}_c)_{\text{lab}}$,

$$\frac{s'}{s} \to \frac{(p_c)_{\parallel}-E_c}{\mu} \equiv -x$$

and (1)

$$\frac{M^2}{s'} = \frac{x-1}{x} \equiv k.$$

The variable x above is just the Feynman scaling variable (Ref. 1) when all transverse momenta are bounded, an assumption that we do not explicitly need. We will find it convenient to use s', t, and k as the independent scalars, where, in the fragmentation domain t and k remain finite as s (and hence $-s'$) tend to infinity.

The high-energy inclusive distribution for the particle c is given by

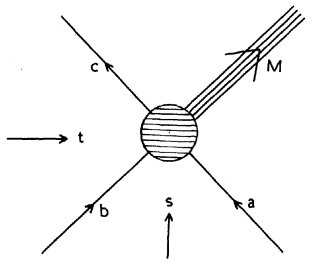

FIG. 1. The inclusive reaction $a + b \to c +$ (anything) and the definition of the related variables.

$$E_c \frac{d\sigma}{dp_c} \propto \frac{1}{s} \operatorname{Im}\langle a(p_a), b(p_b), \bar{c}(-p_c);\text{out}|a(p_a), b(p_b), \bar{c}(-p_c);\text{in}\rangle . \tag{2}$$

For the amplitude $ab\bar{c} \to ab\bar{c}$, we sum all ladder graphs of the type shown in Fig. 2, where the external initial (final) leg $-p_c$ can be attached anywhere on the lower (upper) horizontal line. The crucial indices in the diagram are m, the number of rungs to the left of both $-p_c$ lines, l the number of rungs in between the two $-p_c$ lines, and n the number to the right of both $-p_c$ lines. The special case when $l=0$, i.e., when both $-p_c$ lines are attached to the same box has a more appealing physical interpretation than cases where $l>0$ (see subsequent discussion), but our method will accommodate all values of l. The amplitude we calculate is the sum of all graphs of the type in Fig. 2, with m, l, and n varying independently, and all the way to infinity.

The contribution of any one diagram, corresponding to a given m, l, and n (Fig. 2), is an integral over the internal loop momenta. This can be immediately converted to an integral over the Feynman variables associated with each internal line. The integrations over the loop four-momenta are performed by the

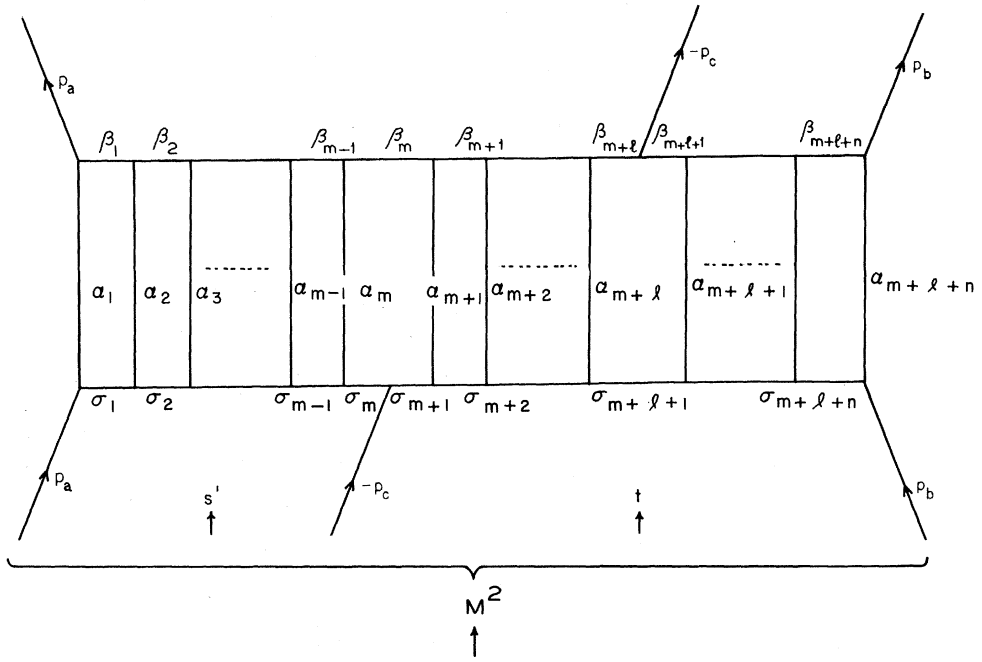

FIG. 2. A typical ladder diagram contributing to the forward amplitude $ab\bar{c}$; out $\to ab\bar{c}$; in. The α_i, β_i, and σ_i are the Feynman parameters associated with the internal lines. The total number of "rungs" is $m+l+n$, of which the first m are to the left of both $-p_c$ external lines, the next l between the two $-p_c$ lines, and the last n to the right of both $-p_c$ lines.

well-known techniques [6] giving

$$A_{m,l,n}(s',t,k)=B\left(\frac{-g^2}{16\pi^2}\right)^{m+l+n+1}(m+l+n+1)!\int_0^1\prod_i d\xi_i\,\frac{\delta(\sum_i\xi_i-1)[C(\xi_i)]^{m+l+n}}{[D(\xi_i,s',t,k)]^{m+l+n+2}}\quad . \tag{3}$$

B contains all inessential constants, common to all diagrams. Here ξ_i refers to the collection of *all* the Feynman variables α_i, β_i, and σ_i shown in Fig. 2. The denominator functions D and C are obtained by using well-known rules which result from the loop-momentum integrations. These rules are succinctly presented in Ref. 6 and we will not repeat them here. Nor do we need to present in their entirety the lengthy expressions for C and D that result from these rules, but merely note their relevant properties. At this stage we note, as can be checked from the application of the above-mentioned rules to this diagram, that:

(a)

$$D=\alpha_1\alpha_2\cdots\alpha_m[\Delta_1(\xi_i)]\,s'+\alpha_1\alpha_2\cdots\alpha_{m+l+n}M^2 +\Delta_2(\xi_i,t,\mu^2)-\left(\sum_i\xi_i\right)C(\xi_i)\mu^2\,. \tag{4}$$

(b) C is a function of the ξ_i alone, and not of s', t, or M^2.

(c) D and C are homogeneous in the ξ_i of degrees $(m+l+n)$ and $(m+l+n-1)$, respectively.

(d) $\Delta_1(\xi_i)$ depends only on α_i, β_i, and σ_i for $i>m$. Further, it will vanish only if *more than one* of these variables vanish. We now proceed to evaluate Eq. (3) in the fragmentation limit viz. fixed $(\vec{p}_c)_{\rm lab}$ as $s\to\infty$. Equation (1) shows that this corresponds to fixed t and fixed $M^2/s'\equiv k$, as $s'\to-\infty$. Consequently, we write the coefficient of s' in the function D [Eq. (4)] as

$$g(\xi_i,k)\equiv[\Delta_1(\xi_i)+k\,\alpha_{m+1}\cdots\alpha_{m+l+n}]\alpha_1\cdots\alpha_m \equiv\alpha_1\alpha_2\cdots\alpha_m f(\xi_i,k)\,. \tag{5}$$

Now, as $s'\to-\infty$, the leading contributions to Eq. (3) will arise from the region of ξ space where $g(\xi_i,k)$ is nearly zero. This can be achieved by the vanishing of one or more of $\{\alpha_1,\ldots,\alpha_m\}$ and/or the vanishing of $f(\xi_i,k)$. However, unlike the region where α_1, $\alpha_2,\ldots,$ or α_m vanish, the region where $f(\xi_i,k)$ vanishes will not enhance the asymptotic behavior in s'. This is because, as per the property of $\Delta_1(\xi_i)$ mentioned above, $f(\xi_i,k)=0$ only if *more* than one ξ_i vanishes. Let us suppose that at least r of ξ_i have to vanish when $f(\xi_i,k)=0$. Let us call them $\xi^{(1)},\ldots,\xi^{(r)}$ (these may include some α's, β's, and some σ's). Let us change variables to $\bar{\xi}^{(i)}=\rho^{-1}\xi^{(i)}$, $i=1,2,\ldots,r$. The simultaneous vanishing of all $\xi^{(i)}$ amounts to $\rho\to0$. But

$$\prod_1^r(d\xi^{(i)})=\rho^{r-1}d\rho\,\delta\left(\sum_i\bar{\xi}^{(i)}-1\right)\prod_1^r(d\bar{\xi}^{(i)})$$

while $f(\xi_i,k)$ and hence $g(\xi_i,k)$ will vanish only linearly with ρ. Consequently, the presence of the ρ^{r-1} factor in the Jacobian above will dilute the contribution of the integral near $\rho=0$, in contrast to the case when any one of the $\{\alpha_1,\ldots,\alpha_m\}$ is near zero. The argument sketched here has been elaborated for other examples in Ref. 6.

Thus, the asymptotically leading terms as $s'\to-\infty$ in Eq. (3) come only from that region where one or more of the set $\{\alpha_1,\ldots,\alpha_m\}\sim0$. The other "rung" variables $\alpha_{m+1},\ldots,\alpha_{m+l+n}$ do not have this significance. Now, *the* leading term will come from the region where *all* the variables in the set $\{\alpha_1,\ldots,\alpha_m\}$ vanish. Then,

$$A_{m,l,n}(s',t,k)\underset{s'\to-\infty}{\sim}B(m+l+n+1)!\left(-\frac{g^2}{16\pi^2}\right)^{m+l+n+1}\int_0^t\prod_1^m(d\alpha_i)\int_0^1\prod_1^{m+l+n}(d\beta_i\,d\sigma_i)\prod_{m+1}^{m+l+n}(d\alpha_i)$$
$$\times\frac{\delta(\sum\xi_i-1)[C(\xi_i)]^{m+l+n}}{[\alpha_1\cdots\alpha_m f(\xi_i,k)s'+\Delta_2(\xi_i,\mu^2,t)-(\sum\xi_i)C(\xi_i)\mu^2]^{m+l+n+2}}$$
$$=B\frac{(\ln s')^{m-1}}{s'(m-1)!}\left(-\frac{g^2}{16\pi^2}\right)^{m+l+n+1}(m+l+n)!\int_0^1\prod_{m+1}^{m+l+n}(d\alpha_i)\prod_1^{m+l+n}(d\beta_i\,d\sigma_i)$$
$$\times\frac{\delta(\sum_i'\xi_i-1)[C'(\xi_i)]^{m+l+n}}{f(\eta,k)[d'(\xi_i,t,\mu^2)]^{m+l+n+1}}\,, \tag{6}$$

where

$$d'(\xi_i,t,\mu^2)=D|_{\alpha_1=\alpha_2=\cdots=\alpha_m=0}\,,$$

$$C'(\xi_i)=C(\xi_i)|_{\alpha_1=\alpha_2=\cdots=\alpha_m=0}\,,$$

$$\sum_i'(\xi_i)=\sum_i(\xi_i)|_{\alpha_1=\alpha_2=\cdots=\alpha_m=0}\,,$$

and $\eta \equiv \{\eta_i\}$ stands for the variables α_i $(i>m)$, β_i $(i>m-1)$, σ_i $(i>m-1)$.

These are the variables to the right of the rung α_m in the diagram. Now we note from the original structure of the C and D functions that

$$C'(\xi)=\left(\prod_{j=1}^{m-1}(\beta_j+\sigma_j)\right)C_1(\eta_i)$$

and (7)

$$d'(\xi_i, t, \mu^2)=\left(\prod_{j=1}^{m-1}(\beta_j+\sigma_j)\right)[\delta_1(t, \mu^2, \eta_i)-(\sum{}'\xi_i)C_1(\eta_i)\mu^2].$$

The homogeneity properties of these functions are

$$f(\rho\eta, k)=\rho^{l+n}f(\eta, k), \qquad C_1(\rho\eta)=\rho^{l+n}C_1(\eta),$$

and (8)

$$\delta_1(t, \mu^2, \rho\eta)=\rho^{l+n+1}\delta_1(t, \mu^2, \eta).$$

Next, we perform the following scale transformations,

$$\beta_j=\rho_j\bar{\beta}_j, \quad \sigma_j=\rho_j\bar{\sigma}_j, \quad 1\leq j\leq m-1$$

and

$$\eta_i=\rho\bar{\eta}_i,$$

so that

$$\prod_{j=1}^{m-1}(d\beta_j d\sigma_j)=\prod_{j=1}^{m-1}[\rho_j d\rho_j d\bar{\beta}_j d\bar{\sigma}_j\delta(\bar{\beta}_j+\bar{\sigma}_j-1)]$$

and

$$d\eta=\rho^{3l+3n+1}d\rho d\bar{\eta}\delta(\sum\bar{\eta}-1).$$

Substituting these in the expression for $A_{m,l,n}(s', t, k)$, we get

$$\begin{aligned}
&A_{m,l,n}(s', t, k)\\
&=B\left(\frac{-g^2}{16\pi^2}\right)^{m+l+n+1}\frac{(m+l+n)!}{(m-1)!}\frac{(\ln s')^{m-1}}{s'}\\
&\times\int_0^\infty\frac{d\rho_1\cdots d\rho_{m-1}d\rho\,\rho^{l+n+1}\delta(\rho_1+\cdots+\rho_{m-1}+\rho-1)\prod_1^{m-1}[d\bar{\beta}_j d\bar{\sigma}_j\delta(\bar{\beta}_j+\bar{\sigma}_j-1)]d\bar{\eta}\,\delta(\sum\bar{\eta}-1)[C_1(\bar{\eta})]^{m+l+n}}{f(\bar{\eta}, k)(\sum_{j=1}^{m-1}h_j\rho_j+h\rho)^{m+l+n+1}}\\
&=B\left(\frac{-g^2}{16\pi^2}\right)^{m+l+n+1}(-)^{l+n+1}\frac{(\ln s')^{m-1}}{s'}\\
&\times\frac{\partial^{l+n+1}}{\partial h^{l+n+1}}\int_0^1\frac{d\rho_1\cdots d\rho_{m-1}d\rho\,\delta(\sum_1^{m-1}\rho_i+\rho-1)\prod_1^{m-1}[d\bar{\beta}_j d\bar{\sigma}_j\delta(\bar{\beta}_j+\bar{\sigma}_j-1)]d\bar{\eta}\,\delta(\sum\bar{\eta}-1)[C_1(\bar{\eta})]^{m+l+n}}{f(\bar{\eta}, k)(\sum_1^{m-1}h_j\rho_j+h\rho)^m},
\end{aligned} \tag{9}$$

where

$$h_j(\bar{\eta})=-C_1(\bar{\eta})\mu^2, \qquad h(\bar{\eta}, t)=\delta_1(t, \mu^2, \bar{\eta})-C_1(\bar{\eta})\mu^2,$$

and we have dropped the factors $(\bar{\beta}_j+\bar{\sigma}_j)$ and $(\sum\bar{\eta})$ because of the δ functions in the numerator.

Performing the $\rho_1, \ldots, \rho_{m-1}$ and ρ integrations with the help of the Feynman identity, we get

$$\begin{aligned}
A_{m,l,n}(s', t, k)&=B\left(\frac{-g^2}{16\pi^2}\right)^{m+l+n+1}(-)^{l+n+1}\frac{(\ln s')^{m-1}}{s'(m-1)!}\\
&\times\frac{\partial^{l+n+1}}{\partial h^{l+n+1}}\int_0^1\frac{\prod_1^{m-1}[d\bar{\beta}_j d\bar{\sigma}_j\delta(\bar{\beta}_j+\bar{\sigma}_j-1)]d\bar{\eta}\,\delta(\sum\bar{\eta}-1)[C_1(\bar{\eta})]^{m+l+n}}{f(\bar{\eta}, k)(-\mu^2)^{m-1}[C_1(\bar{\eta})]^{m-1}h(\bar{\eta}, t)}\\
&=B\left(\frac{-g^2}{16\pi^2}\right)^{m+l+n+1}\frac{(\ln s')^{m-1}}{s'(m-1)!}(l+n+1)!
\end{aligned}$$

$$\times\left(\int_0^1 \frac{d\bar{\eta}\,\delta(\sum\bar{\eta}-1)[C_1(\bar{\eta})]^{l+n+1}}{f(\bar{\eta},k)[h(\bar{\eta},t)]^{l+n+2}}\right)\prod_{j=1}^{m-1}\left(\int_0^1\frac{d\bar{\beta}_j d\bar{\sigma}_j\delta(\bar{\beta}_j+\bar{\sigma}_j-1)}{(-\mu^2)}\right)$$

$$=B\frac{(\ln s')^{m-1}}{s'(m-1)!}K^{m-1}\Gamma_{l,n}(k,t), \tag{10}$$

where

$$K=\left(\frac{-g^2}{16\pi^2}\right)\int_0^1\frac{d\bar{\beta}_j d\bar{\sigma}_j\delta(\bar{\beta}_j+\bar{\sigma}_j-1)}{(-\mu^2)}$$

$$=\frac{g^2}{16\pi^2\mu^2} \tag{11}$$

and

$$\Gamma_{l,n}(k,t)=\left(\frac{-g^2}{16\pi^2}\right)^{l+n+2}(l+n+1)!\int_0^1\frac{d\bar{\eta}\,\delta(\sum\bar{\eta}-1)[C_1(\bar{\eta})]^{l+n+1}}{f(\bar{\eta},k)[h(\bar{\eta},t)]^{l+n+2}}\ . \tag{12}$$

Thus, the coefficient of $(\ln s')^{m-1}/s'$ in $A_{m,l,n}(s',t,k)$ factorizes into m terms. This factorization is pictorially depicted in Fig. 3. The first $(m-1)$ factors are each equal to K, which corresponds to one "bubble" in Fig. 3. Note that in ladder models for four-point functions in this same $g\phi^3$ theory,[6] the *forward* elastic $(2\to 2)$ amplitude will contain these same factors K. The last factor $\Gamma_{l,n}$ depends only on k and t, i.e., $(\vec{p}_c)_{\rm lab}$, and it involves integrations only over the variables η, which are to the right of the α_m rung.

Summing $A_{m,l,n}(s',t,k)$ over all m, l, and n,

$$A(s',t,k)\equiv\sum_{m,l,n}A_{m,l,n}(s',t,k)$$

$$\underset{s'\to\infty}{\sim}\frac{B}{s'}\left(\sum_m\frac{(K\ln s')^{m-1}}{(m-1)!}\right)\left(\sum_{l,n}\Gamma_{l,n}(k,t)\right)$$

$$=B(s')^{K-1}\bar{\Gamma}(k,t), \tag{13}$$

where

$$\bar{\Gamma}(k,t)=\sum_{l,n}\Gamma_{l,n}(k,t).$$

Thus, we see that the summation of all ladder diagrams of the type in Fig. 2 gives a Regge-behaved amplitude in the variable $s'=-xs$. The trajectory $K-1$ is identical to that arising in the elastic case, since the same expression for K comes in here. Note that since we are dealing with a forward $ab\bar{c}\to ab\bar{c}$ amplitude, there are no momentum-transfer variables in the process and K is just a number. Thus $K-1$ is the trajectory function at zero momentum transfer for elastic scattering. If we identify it with the Pomeranchukon, we can set $K-1=1$. We then have

$$E_c\frac{d\sigma}{d\vec{p}_c}\propto\frac{1}{s}\,\mathrm{Im}A(s',t,k)$$

$$\propto\bar{\Gamma}\left(\frac{M^2}{s'},t\right)(-x).$$

Thus, limiting fragmentation is achieved.[7] The

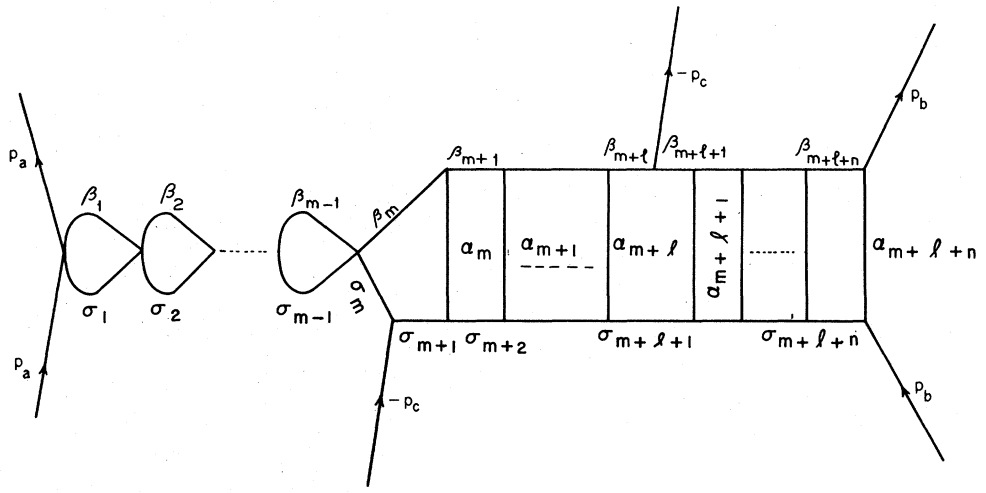

FIG. 3. The factorization property of the coefficient of the leading $(\ln s')^{m-1}/s'$ term in $A_{m,l,n}$.

Regge residue function $\bar{\Gamma}$ depends only on $(\vec{p}_c)_{\text{lab}}$ as can be seen from Eq. (1) for t and $M^2/s' = k$.

Although the leading-term approximation used above Reggeizes and can give limiting fragmentation, the fragment distribution function $\bar{\Gamma}(M^2/s', t)(-x)$ is still ambiguous in this method. To see this, let us suppose that one had chosen to use M^2 instead of s' as the variable tending to infinity with $s'/M^2 = 1/k$. Following all the steps above, one would end up with the result:

$$A(s', t, k) \underset{\substack{M^2\to\infty \\ t \text{ and } s'/M^2 \text{ fixed}}}{\sim} B(M^2)^{K-1}\bar{\Gamma}\left(\frac{M^2}{s'}, t\right)\frac{M^2}{s'} = \left[Bs'^{K-1}\bar{\Gamma}\left(\frac{M^2}{s'}, t\right)\right]\left(\frac{M^2}{s'}\right)^K .$$

This new Regge residue, and hence the limiting distribution function, has changed by a factor $(M^2/s')^K$ even though the physical limit is the same as before. Such an ambiguity of the Regge residue is a manifestation of the defective nature of the leading-term approximation, which while it retains the $(1/s')(\ln s')^{m_0-1}$ term for $m = m_0$, ignores similar terms from diagrams where $m > m_0$. Such a problem exists in the elastic case as well where, even though the result will Reggeize, the residue function is quite arbitrary. Its momentum transfer dependence can be altered by a trivial change of variables. Correspondingly, in our inclusive reaction case, the leading-term method cannot predict the limiting distribution function uniquely.

This motivates us in Sec. III to perform an exact summation of these ladder terms. The work of Sec. II however gives much insight into the problem and makes the presentation of Sec. III simpler.

III. THE MELLIN-TRANSFORM METHOD

In this section, we do away with the unsatisfactory approximation of neglecting terms lower than $(1/s')(\ln s')^{m-1}$ in $A_{m,l,n}(s', t, k)$. This is done by performing a Mellin transform on $A_{m,l,n}(s', t, k)$, summing over m, l, and n, and then performing an inverse transform on the result. We have,

$$A_{m,l,n}(s', t, k) = B\left(\frac{-g^2}{16\pi^2}\right)^{m+l+n+1}(m+l+n+1)!\int_0^1 \frac{\prod_i (d\xi_i)\delta(\sum_i \xi_i - 1)[C(\xi_i)]^{m+l+n}}{[D(\xi_i, s', t, k)]^{m+l+n+2}} . \tag{14}$$

We keep k and t fixed as before, and let $s' \to -\infty$. When $s' \to -\infty$, the function D is negative definite, and C is positive definite for positive ξ_i. Using this, and the homogeneity properties of C and D mentioned in Sec. II, we can convert Eq. (14) to [5]

$$A_{m,l,n}(s', t, k) = B\left(\frac{-g^2}{16\pi^2}\right)^{m+l+n+1}(-)^{m+l+n}\int_0^\infty \prod_i (d\xi_i)\frac{\exp[D(\xi_i, s', t, k)/C(\xi_i)]}{[C(\xi_i)]^2} . \tag{15}$$

Now, from Eqs. (4) and (5), we write

$$D(\xi_i, s', t, k) = -g(\xi_i, k)(-s') - J(\xi_i, t)C(\xi_i), \tag{16}$$

where

$$J(\xi_i, t) = -\frac{\Delta_2(\xi_i, t, \mu^2)}{C(\xi_i)} + \left(\sum_i \xi_i\right)\mu^2 .$$

Taking the Mellin transform of Eq. (15) with respect to $(-s')$,

$$A_{m,l,n}(\beta, t, k) = \int_0^\infty (-s')^{-\beta-1}A_{m,l,n}(s', t, k)d(-s') = B\left(\frac{-g^2}{16\pi^2}\right)^{m+l+n+1}\Gamma(-\beta)(-)^{m+l+n}\int_0^\infty \prod_i (d\xi_i)\frac{[g(\xi_i, k)]^\beta}{[C(\xi_i)]^{2+\beta}}\exp[-J(\xi_i, t)] . \tag{17}$$

The function $g(\xi_i, k)$ has the form [Eq. (5)]

$$g(\xi_i, k) = \alpha_1\alpha_2\cdots\alpha_m f(\eta, k),$$

where the variables η have been defined in Eq. (7). It has already been seen in Sec. II that the variables $\{\alpha_1, \ldots, \alpha_m\}$ have a special significance as distinct from the other α's or the β's and σ's in that they give the leading behavior to $A_{m,l,n}(s', t, k)$ when they are near zero. The same fact manifests itself here. The integral in Eq. (17) is singular at $\beta = -1$ because of the $(\alpha_1\alpha_2\cdots\alpha_m)^\beta$ factor in $[g(\xi_i, k)]^\beta$. The $[f(\eta, k)]^\beta$ does not produce a singularity at $\beta = -1$, though it *can* vanish, since such vanishing requires more than one η variable to be zero. In this sense the $[f(\eta, k)]^\beta$ factor is similar to the $[C(\xi_i)]^{-\beta}$ factor in Eq. (17) and and can be combined with it. Then the singularity at $\beta = -1$ can be exhibited explicitly by integrating Eq. (17) by parts to give

$$A_{m,l,n}(\beta,t,k)=B\Gamma(-\beta)\left(\frac{-g^2}{16\pi^2}\right)^{m+l+n+1}(-)^{l+n}\int_0^\infty\frac{(\alpha_1\alpha_2\cdots\alpha_m)^{\beta+1}}{(\beta+1)^m}\frac{\partial^m}{\partial\alpha_1\cdots\partial\alpha_m}\left[\frac{e^{-J(\xi_i,t)}}{C(\xi_i)f(\eta,k)}\left(\frac{f(\eta,k)}{C(\xi_i)}\right)^\beta\right]\prod_i(d\xi_i). \tag{18}$$

Thus $A_{m,l,n}(\beta,t,k)$ has been reduced to the same form that appears in the elastic problem [Eq. (3.6.15) in Ref. 6] and the rest of the steps follow through in a manner identical to that problem. The only difference as compared to the elastic case is that of all the rungs $\alpha_1,\alpha_2,\ldots,\alpha_{m+l+n}$, only the first m rungs contribute to the pole at $\beta=-1$ and the function $[f(\eta,k)/C(\xi_i)]^{\beta+1}$ replaces $[C(\xi_i)]^{-\beta-1}$. We outline the subsequent steps very briefly. The mth-order pole at $\beta=-1$ gives the leading term discussed in Sec. II. We keep here all the lower-order poles as well and the nonsingular terms by expanding the coefficient of $\Gamma(-\beta)/(\beta+1)^m$ in Eq. (18) in powers of $(\beta+1)$. This gives

$$A_{m,l,n}(\beta,t,k)=B\Gamma(-\beta)\left(\frac{-g^2}{16\pi^2}\right)^{m+l+n+1}(-)^{l+n}$$
$$\times\sum_{p=-\infty}^{m}\sum_{q=0}^{m-p}\sum_{s_j}\int_0^\infty\prod_i(d\xi_i)\prod_{j=1}^{m}\frac{(\ln\alpha_j)^{s_j}}{s_j!}\frac{\partial^m}{\partial\alpha_1\cdots\partial\alpha_m}\left(\frac{e^{-J}}{Cf}\frac{[(\ln(f/C)]^q}{q!}\right)\frac{1}{(\beta+1)^p}, \tag{19}$$

where the sum over s_j is over all sets of integers s_j satisfying $\sum_j s_j=m-p-q$. When some of the s_j are zero, the integration over those α_j is trivial and amounts to setting those $\alpha_j=0$ in the terms inside the large round parentheses. Further, the expressions e^{-J}, f, and C factorize as depicted in Fig. 4. In Fig. 4, $j_1,\ldots,j_r$ stands for those indices $j_i\le m$ which have $s_j=0$. The term $(\ln f/C)$ is now a sum of independent terms, so that each term in the multinomial expansion for $[\ln(f/C)]^q$ is factorized in the sense of Fig. 4. We also sum Eq. (19) over the index m. Then exactly as in the elastic case $\sum_m A_{m,l,n}(\beta,t,k)$, which is a sum of factorized terms, will again factorize. We merely quote the result:

$$\sum_m A_{m,l,n}(\beta,t,k)=\Gamma(-\beta)G^{(1)}(\beta)\frac{1}{F(\beta)}G^{(2)}_{l,n}(\beta,t,k),$$

where

$$G^{(1)}(\beta)=\sum_{j=0}^{\infty}\bar{G}^{(1)}_j(\beta),$$
$$F(\beta)=-\left(\sum_{j=0}^{\infty}\bar{F}_j(\beta)\right)+\beta+1, \tag{20}$$
$$G^{(2)}_{l,n}(\beta,t,k)=\sum_{j=0}^{\infty}\bar{G}^{(2)}_{j,l,n}(\beta,t,k).$$

Here,

$$\bar{G}^{(1)}_j(\beta)=-g\left(\frac{-g^2}{16\pi^2}\right)^j\int_0^\infty d\alpha_1\cdots d\alpha_j\prod_i(dy_i^{(1)})\prod_{r=1}^{j}\left(\frac{\alpha_r^{\beta+1}-1}{\beta+1}\right)\frac{\partial^j}{\partial\alpha_1\cdots\partial\alpha_j}\left(\frac{e^{-J_j^{(1)}}}{(C_j^{(1)})^{2+\beta}}\right), \tag{21a}$$

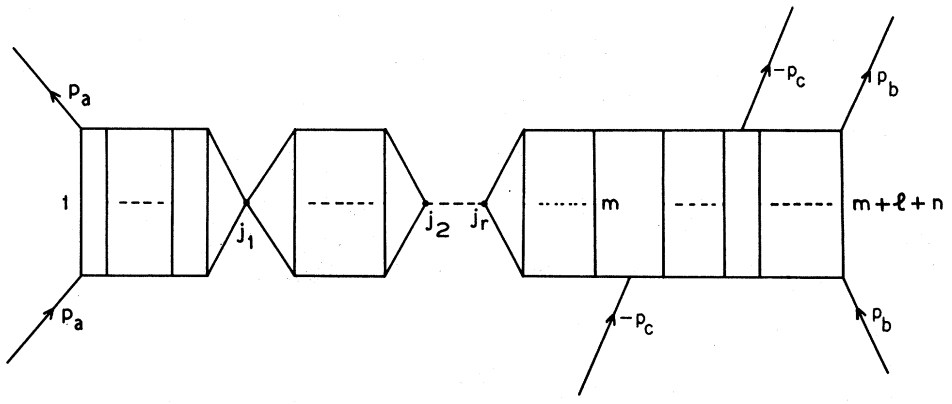

FIG. 4. The factorization property of Eq. (19) when the powers s_j of the $(\ln\alpha_j)$ are zero for $j=j_1,\ldots,j_r$. Here the set $(j_1,\ldots,j_r)$ is a subset of $(1,\ldots,m)$.

$$\bar{F}_j(\beta) = -\left(\frac{-g^2}{16\pi^2}\right)^{j+1} \int_0^\infty d\alpha_1 \cdots d\alpha_j \prod_i (dy_i) \prod_{r=1}^{j} \left(\frac{\alpha_r^{\beta+1}-1}{\beta+1}\right) \frac{\partial^j}{\partial\alpha_1 \cdots \partial\alpha_j} \left(\frac{e^{-J_j}}{(C_j)^{2+\beta}}\right), \tag{21b}$$

$$\bar{G}^{(2)}_{j,l,n}(\beta, t, k) = \left(\frac{-g^2}{16\pi^2}\right)^{j} B_{l,n} \int_0^\infty d\alpha_1 \cdots d\alpha_j \prod_i (dy_i^{(2)}) \prod_{r=1}^{j} \left(\frac{\alpha_r^{\beta+1}-1}{\beta+1}\right) \frac{\partial^j}{\partial\alpha_1 \cdots \partial\alpha_j} \left(\frac{\exp[-J^{(2)}_{j,l,n}(\xi, t)][f(\eta, k)]^\beta}{[C^{(2)}_{j,l,n}(\xi)]^{2+\beta}}\right). \tag{21c}$$

The factor $\bar{G}^{(1)}_j$ is depicted in Fig. 5(a). The functions $J^{(1)}_j$ and $C^{(1)}_j$ correspond to the diagram in Fig. 5(a) as per their definitions and the rules for obtaining them. Similarly, J_j, C_j, and $\bar{F}_j$ correspond to Fig. 5(b) and $J^{(2)}_{j,l,n}$, $C^{(2)}_{j,l,n}$, and $\bar{G}^{(2)}_{j,l,n}(\beta, t, k)$ correspond to Fig. 5(c). Note that $\bar{G}^{(1)}_j = g$ for $j = 0$, while $\bar{G}^{(2)}_{j,l,n}$ for $j = 0$ is still an integral involving all the variables η_i. The integration variables $y^{(1)}_i$, y_i, and $y^{(2)}_i$ refer to all the

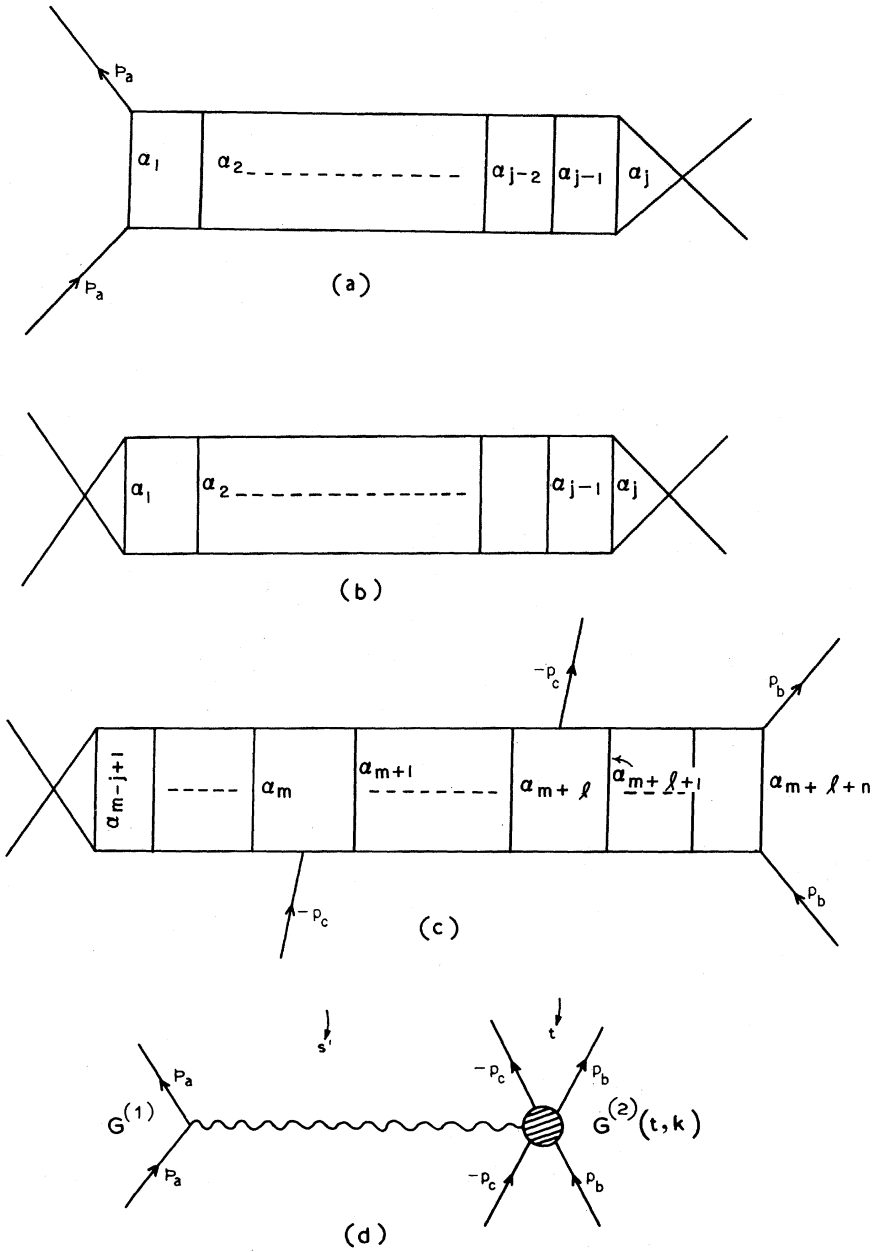

FIG. 5. (a) The factor $\bar{G}^{(1)}_j(\beta)$ defined in Eq. (21a). Similarly, (b) and (c) correspond to $\bar{F}_j(\beta)$ and $\bar{G}^{(2)}_{j,l,n}$, respectively. (d) gives the resulting Regge-pole behavior with the factorized residue $G^{(1)}(\beta) G^{(2)}(\beta, t, k)$.

variables in the corresponding diagram except for $\alpha_1, \ldots, \alpha_j$, which are explicitly shown. When the Mellin transform $\sum_m A_{m,l,n}(\beta, t, k)$ in Eq. (20) is inverted, the resulting amplitude $\sum_m A_{m,l,n}(s', t, k)$ will show Regge behavior corresponding to the zeros of $F(\beta)$. If these zeros are at $\beta = \beta_i$, the high-energy amplitude is

$$\sum_m A_{m,l,n}(s', t, k) \underset{s' \to -\infty}{\sim} \sum_i \Gamma(-\beta_i) G^{(1)}(\beta_i) G^{(2)}_{l,n}(\beta_i, t, k) \times \text{Residue}\left(\frac{1}{F(\beta)}\right)_{\beta=\beta_i} (-s')^{\beta_i} . \tag{22}$$

Note that just as in the leading-term approximation, summation over l and n is not necessary for Regge behavior, although such summation can be performed for completeness. This would merely replace $G^{(2)}_{l,n}(\beta_i, t, k)$ by

$$\sum_{l,n} G^{(2)}_{l,n}(\beta_i, t, k) \equiv G^{(2)}(\beta_i, t, k)$$

in Eq. (22).

The residue of each Regge pole factorizes nicely. The factor $G^{(1)}(\beta_i)$ can be considered as the $(a\text{-}a)$-Reggeon vertex, and is composed of ladders at the left extremity of the diagram [Fig. 5(a)]. The factor $G^{(2)}(\beta_i, t, k)$ represents the $(b\bar{c}\text{-}b\bar{c})$-Reggeon vertex, and contains all the dependence on t and k, and hence $(\vec{p}_c)_{\text{lab}}$. Both the Regge vertices are at zero momentum transfer since the forward $ab\bar{c} \to ab\bar{c}$ is involved. Hence $G^{(1)}(\beta_i)$ and $\Gamma(-\beta_i)$ are just numbers. We have taken the zeros of $F(\beta)$ to be linear. If higher zeros are present, Eq. (22) is modified in an obvious way.

Finally, the function $F(\beta)$ whose zeros give the Regge trajectories, is a sum of terms of the type depicted in Fig. 5(b) and explicitly shown in Eq. (21b). It may be seen that this function is exactly the same as that arising in the Mellin-transform treatment of elastic forward $ab \to ab$ scattering in the same ϕ^3 theory. Consequently, the trajectories in the fragmentation limit of the forward $ab\bar{c} \to ab\bar{c}$ amplitude are the same as those in the forward $ab \to ab$ amplitude. This identification, involved in O(2,1) models of inclusive reactions, is thus supported in ϕ^3 theory. Consequently, the leading trajectory corresponding to the Pomeranchukon will have $\beta = 1$, giving limiting fragmentation. There is a technical problem in as much as the $\beta_i = 1$ term in Eq. (22) is purely real, and further $\Gamma(-\beta)$ has a pole at $\beta = 1$. As in conventional Regge theory, both these problems are overcome by the introduction of the signature factor. This can be done in our ladder model as well. For this, we merely add to our sequence of diagrams, the corresponding set where the two external lines p_a are crossed. It can be easily seen that this added set corresponds to $s' \to -s'$, with the same k and t. Thus, addition of this set amounts to a factor $(1 + e^{i\pi\beta_i})$ in each term of Eq. (22). This factor nullifies the pole of $\Gamma(-\beta_i)$ as $\beta_i \to +1$ and further renders that term fully imaginary. With this modification, the leading $\beta = 1$ term contribution in Eq. (22) gives

$$\lim_{s \to \infty;\, t, M^2/s \text{ fixed}} E_c \frac{d\sigma}{d\vec{p}_c} \propto \frac{1}{s} \text{Im}\langle a, b, \bar{c};\ \text{out} | a, b, \bar{c};\ \text{in}\rangle \propto x G^{(2)}(\beta, t, k)|_{\beta=1} = \sum_{l,n} x G^{(2)}_{l,n}(\beta, t, k)|_{\beta=1} . \tag{23}$$

This gives us limiting fragmentation as well as the limiting distribution itself. Since no leading-term approximation is made in this result, the residue $G^{(1)} G^{(2)}$ in Eq. (22) is unambiguous so that Eq. (23) for the limiting distribution as a function of $\vec{p}_c$ is an exact result of the model. In principle, given the mass μ and the coupling constant g, one can evaluate the distribution from Eqs. (20), (21c), and (23). In fact, since the leading trajectory function is set by hand to be unity, the leading zero of $F(\beta)$ in Eq. (20) must be at $\beta = 1$. This gives an added constraint connecting μ and g.

However, the expressions for $F(\beta)$ and $G^{(2)}(\beta, t, k)$ are sufficiently complicated so that there seems no simple way of exploiting these relations to give a more explicit form for the limiting distribution than Eq. (23) itself. We are currently exploring the properties of the integrals in Eq. (23) in an attempt to extract at least some features of the t and k dependence.

We conclude with some remarks about the choice of the diagrams (Fig. 2) that defined our model. First consider the case when $l = 0$ in Fig. 2. The discontinuity in M^2 of the diagram is then just the absolute square of the well known multiperipheral chain for the $a + b \to$ (many particles) amplitude, with all final particles except c integrated over. Further, if the external lines $-p_c$ were joined and integrated over, one obtains the familiar planar ladder graph for the elastic $ab \to ab$ process. Thus, the choice of Fig. 2 for our model is a physically appealing one when $l = 0$, with arbitrary m and n.

When $l > 0$, Fig. 2 still has an acceptable interpretation. When the $-p_c$ lines are joined the resulting graph for $ab \to ab$ shown in Fig. 6(a) is the ladder diagram with the line c crossed across l other rungs. The discontinuity in s of Fig. 6(a) gives the product of a "direct" Amati-Bertocchi-Fubini-Stanghellini-Tonin (ABFST) graph for the $ab \to$ (many particles) process with an exchange

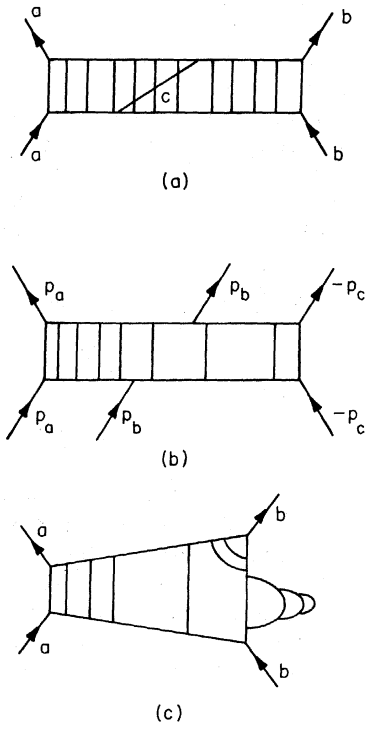

FIG. 6. (a) The elastic amplitude corresponding to joining the external lines $-p_c$ in Fig. 2 and integrating over p_c. (b) is similar to Fig. 2 except that the external lines p_b and $-p_c$ have interchanged their positions. This graph corresponds to bremsstrahlung emission by particle b. (c) is the result of joining the external lines $-p_c$ in (b).

graph for the same process. In general such terms are expected to be there in perturbation theory, but a complete set of direct and exchange terms would lead to crossing *all* the rungs in Fig. 6(a) (and Fig. 2) in all possible ways – a complication that our techniques cannot easily handle. Given that diagrams with $l \neq 0$ correspond only to some of the crossed processes and not all, it is not clear if their inclusion will improve the result or not. Of course, our method leads to limiting fragmentation whether l is set equal to zero, or summed over [see Eq. (22)]. But the limiting distribution function [Eq. (23)] will depend on this.

Finally, another interesting set of graphs is obtained [Fig. 6(b)] by exchanging the positions of the external lines b and $\bar{c}$ in Fig. 2. Our techniques are immediately applicable for the sum of these graphs as well. (The variable s' in Fig. 2 is replaced here by s which also tends to infinity while M^2/s and t are kept fixed in the fragmentation limit.) These graphs will once again yield Regge behavior and limiting fragmentation. Their discontinuity in M^2 corresponds to a set of bremsstrahlung particles emitted by b, to which c also belongs, in addition to a multiperipheral chain between a and b. This is clearly another natural source for fragments of b to come from. However, if the external lines $-p_c$ in Fig. 6(b) were joined together, the resulting graph [Fig. 6(c)] for the elastic $ab \to ab$ process involves self-energy and vertex loops and is also divergent. Such graphs clearly have to be renormalized away along with a much larger class of such graphs, and our method is not easily adopted to all of them.

All this discussion shows that while our method can treat for all values of l diagrams in Fig. 2 and Fig. 6(b), which are all legitimate contributors to the full answer for the limiting distribution, these diagrams are a very incomplete set. Perhaps the best place to draw the line is to merely calculate the $l=0$ contribution for Fig. 2, from Eq. (22).

---

[1]J. Benecke, T. T. Chou, C. N. Yang, and E. Yen, Phys. Rev. 188, 2159 (1969); R. P. Feynman, Phys. Rev. Letters 23, 1415 (1969). Feynman's postulate of scaling amounts to "limiting fragmentation" when his scaling variable $x \neq 0$.

[2]See, for example, L. G. Ratner *et al.*, Phys. Rev. Letters 27, 68 (1971).

[3]A. H. Mueller, Phys. Rev. D 2, 2963 (1970).

[4]For a sample, see C. E. DeTar, Phys. Rev. D 3, 128 (1971); D. Gordon and G. Veneziano, *ibid.* 3, 2116 (1971); M. A. Virasoro, *ibid.* 3, 2834 (1971); C. E. DeTar *et al.*, *ibid.* 4, 425 (1971); D. K. Campbell and S.-J. Chang, *ibid.* 4, 3658 (1971).

[5]J. C. Polkinghorne, J. Math. Phys. 4, 503 (1963); I. G. Halliday and J. C. Polkinghorne, Phys. Rev. 132, 274 (1963); J. D. Bjorken and T. T. Wu, *ibid.* 130, 2566 (1963); J. C. Polkinghorne, J. Math. Phys. 5, 431 (1964); Nuovo Cimento 36, 857 (1965). This is not a complete list of references in this area, but familiarity with the above will suffice for reading our paper.

[6]R. J. Eden, P. Y. Landshoff, D. I. Olive, and J. C. Polkinghorne, *The Analytic S-Matrix* (Cambridge Univ. Press, Cambridge, England, 1966). (Our notation here is kept very close to the one used in this book for the convenience of the reader.)

[7]Strictly speaking, the amplitude derived above is real. However, the residue $\bar{\Gamma}(M^2/s, t)$ has considerable ambiguity in this method as the subsequent discussion shows, and the amplitude can accommodate an arbitrary complex constant. In the exact method presented in the next section, this ambiguity is removed, and the imaginary part is seen to arise on adding appropriate crossed graphs. See the discussion at the end of Sec. III.